INTERNATIONAL JOURNAL OF INTEGRATED ENGINEERING
ISSN: 2229-838X e-ISSN: 2600-7916

IJIE

Vol. 17 No. 6 (2025) 27-39
https://publisher.uthm.edu.my/ojs/index.php/ijie

Computational Intelligence and Load to Source Ratio Index Based Technique for Voltage Security Restoration

Muhammad Naqiyuddin Ismail[1], Mazliza Abdul Halim[1]*, Ismail Musirin[1], Vinothini Kasinathan[2], Aida Mustapha[3], Habibah Zulkefle[1]

[1] *School of Electrical Engineering, College of Engineering, Universiti Tekologi MARA, Shah Alam, 40450, MALAYSIA*
[2] *School of Computing, Asean Pacific of University of Technology and Innovation, Kuala Lumpur, 57000, MALAYSIA*
[3] *Faculty of Applied Sciences and Technology, Universiti Tun Hussein Onn Malaysia, KM 1 Jalan Panchor, Panchor, 84600, MALAYSIA*

*Corresponding Author: mazliza@uitm.edu.my
DOI: https://doi.org/10.30880/ijie.2025.17.06.003

Article Info

Received: 11 January 2025
Accepted: 4 July 2025
Available online: 30 December 2025

Keywords

Voltage security, weakest bus, evolutionary programming, computational intelligence, voltage collapse

Abstract

Voltage security remains a critical concern in power systems, as voltage instability can lead to service disruptions and cascading failures. This paper presents an advanced computational intelligence technique based on the load-to-source ratio index, $\boldsymbol{Z_L/X_{Th}}$ integrated with Evolutionary Programming (EP) to enhance voltage stability. Unlike conventional methods, this approach optimizes reactive power dispatch (ORPD) across multiple configurations to improve voltage levels throughout the network. The technique was validated on the IEEE-30 Bus Reliability Test System under various loading conditions. Results show significant improvements in the $\boldsymbol{Z_L/X_{Th}}$ index for weak buses, with an increase from 10.9667 to 24.3144 at the critical Bus 29, leading to improved voltage levels across the system. Additionally, the method offers enhanced flexibility by assessing multiple ORPD scenarios, allowing system operators to choose the optimal configuration for different network conditions. These findings suggest that the proposed method not only improves voltage security but also provides a robust, adaptable solution for practical power system operations.

1. Introduction

Voltage collapse is an unpredictable phenomenon, even when appropriate remedial measures are implemented. If left uncontrolled, the cost of repairs will escalate significantly, leading to substantial financial burdens. In today's modern era, the power system is crucial for society, ensuring the continuity of daily activities. It is inconceivable for a community to function without a reliable electricity supply. Therefore, power supply companies must adhere to customer demands and ensure that energy is provided in accordance with consumption needs.

Statistical data indicates that voltage collapse remains a persistent risk and can occasionally pose threats to public safety and cause equipment damage. Reports suggest that at least five significant disruptions to the global electrical power supply occurred in 2003 [1]. Notable blackout incidents worldwide include: (i) 14th August 2003 at 1610h, affecting the central Canada and northeastern United States, (ii) 28th August 2003 at 18:26pm, impacting central United Kingdom, (iii) 1st September 2003 at 09:58 am, occurring in northern Malaysia, (iv) 23rd September 2003 at 12:35 pm, affecting eastern southern Sweden and Denmark, and (v) 28th September 2003 at 03:28 am, impacting the entirely of southern Switzerland and Italy. These incidents have necessitated

critical remedial measures for voltage restoration. In the process of voltage restoration, disturbances can be classified as either minor or major events. This classification arises from the fact that blackouts typically result from a sequence of events known as cascading voltage collapse. A noteworthy study reported in [2] highlights common factors contributing to blackouts, including: (i) transmission line overloading or generator tripping, (ii) deviations in system frequency, (iii) voltage collapse within the power system, (iv) loss of generator synchronism, and (v) increasing low-frequency oscillations in large power systems.

Voltage collapse has become a significant concern, garnering extensive research attention. Various strategies have been proposed to mitigate power outages effectively. One such approach is a user-centered restoration method, structured into three distinct stages [3]. Additionally, the network and load recovery (NLR) process is divided into two phases to enhance efficiency [4]. Another technique involves segmenting power system restoration into three stages [5]. This study aims to minimize the Standing Phase Angle (SPA) by ensuring synchronization throughout the restoration process [6]. Moreover, the Optimum Power Flow for Distribution System Restoration (OPFDSR) algorithm has been introduced as a potential solution, as discussed in [7].

Furthermore, voltage restoration and power management in DC microgrids have been explored through coordinated droop control, a method that stabilizes a DC microgrid via a virtual voltage axis [8]. The stochastic response surface method (SRSM) has also been introduced to address uncertainty in distributed generation (DG) systems [9]. Additionally, an optimal power flow (OPF)-based algorithm has been developed to facilitate power transfer from a black start unit (BSU) to a non-black start unit (NBSU) [10]. This study also introduces the Teaching-Learning Based Optimization algorithm to solve bi-level optimization problems and determine the optimal sequence for restoring NBS units [11]. Another proposed technique is the elliptical restoration method, which focuses on the transitional phase during power factor correction at the source [12]. Lastly, the restoration process is classified into three categories: (i) DC voltage containment reserve, (ii) DC voltage restoration reserve, and (iii) DC voltage replacement reserve [13].

A load-to-source impedance-based approach, as discussed in [14], has been proposed by other researchers. This method emphasizes the importance of matching load impedance with source impedance to maximize power transfer and identify the system's weakest bus [15], [16]. The proposed technique has been applied to optimize reactive power dispatch, commonly known as ORPD. ORPD plays a vital role in voltage regulation within resilient distribution systems, particularly those with high renewable energy penetration [17].

In this study, the Artificial Bee Colony (ABC) algorithm [18], [19], an artificial intelligence-based technique, was employed to solve the ORPD problem [20]. AI-based methods, including neural networks and reinforcement learning, are increasingly being utilized to enhance voltage stability and power system protection by enabling dynamic control and real-time monitoring [21].

Additionally, extensive research in [19] has examined ORPD solutions using various optimization techniques, including Evolutionary Algorithms (EA), Differential Evolution (DE), and Particle Swarm Optimization (PSO) [20]. A significant advancement in this field is the development of the two-archive Multi-Objective Grey Wolf Optimizer (2ArchMGWO) [22], an improved variant of the Multi-Objective Grey Wolf Optimizer (MGWO), designed to address the Multi-Objective Optimal Reactive Power Dispatch (MORPD) problem. Another notable contribution is the application of the Moth-Flame Optimization (MFO) algorithm for solving ORPD issues [23], [24].

This paper introduces a computational intelligence approach integrated with a load-to-source ratio index-based method for voltage security restoration. Evolutionary Programming (EP) is employed to identify the system's weakest bus under varying load conditions. The identification process is conducted by computing the Z_L/X_{Th} index. A predefined load is assigned, and the load-to-source index for each bus is determined. Once the weakest load bus is identified, EP is utilized to optimize the Optimal Reactive Power Dispatch (ORPD) on generator buses, thereby maximizing the critical index. By enhancing the Z_L/X_{Th} index, the voltage magnitude at the load bus is effectively restored.

2. Methodology

The research methodology employed in this study is illustrated in Fig. 1. The procedure begins with the calculation of the load-to-source ratio impedance index, Z_L/X_{Th}. This index is specifically applied to load buses to identify the weakest load bus during the load flow analysis. Additionally, the general flowchart for Evolutionary Programming is illustrated in Fig. 1.

Int. Journal of Integrated Engineering Vol. 17 No. 6 (2025) p. 27-39

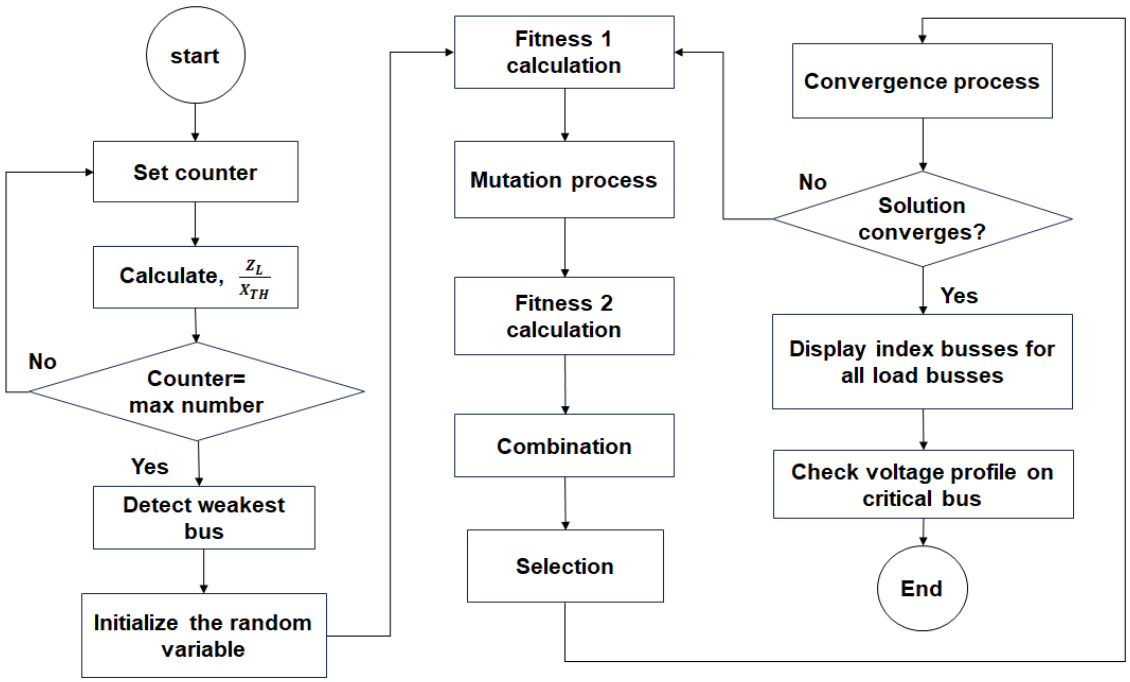

Fig. 1 *Flowchart of evolutionary programming*

Step 1: Set counter:

The counter is initially configured to represent all buses within the test power system. It is then utilized to compute the Z_L/X_{Th} index for each bus. Additionally, a condition is established to ensure that the output is generated exclusively for load buses. In this study, the IEEE-30 bus reliability test system (RTS) was selected for validation purposes.

Step 2: Calculate Z_L/X_{Th} index:

Two conditions are established for calculating the Z_L/X_{Th} index. The first condition is the no-load condition, where both power demand (Pd) and reactive power demand (Qd) are set to zero. After executing the load flow analysis, the obtained voltage magnitude Vk is referred to as V_{oc}, representing the open-circuit voltage when no load is present on the bus. Next, I_{SC} is determined using the 'zbuildpi' and 'symmfault' functions available in the power system toolbox developed by Hadi Saadat [23]. The value of ISC is derived from the calculated fault current. Since only the imaginary component of Z_{Th}, denoted as X_{Th}, is required, the angles of V_{oc} and I_{SC} must be considered before performing the calculation. Equation (1) is used to determine XTh, as follows:

$$X_{TH} = {V_{OC}}/{I_{SC}} \tag{1}$$

X_{Th} = imaginary part of Thevenin impedance
V_{oc} = voltage under open-circuit condition
I_{SC} = current under short-circuited condition
V_k = load bus voltage

In the second condition, the same load is assigned to all load buses, and the load flow analysis is performed again to determine Z_L. Maintaining a uniform load across all load buses is essential for assessing their performance. In this study, the load values were set to P_d = 5 MW and Q_d = 5 MVAR to ensure the load flow converges for all load buses. After executing the load flow analysis, a new value of V_k is obtained, and equations (2), (3), and (4) are used to compute Z_L:

$$S_{d(p.u)} = {\left[{P_d}^2 + {Q_d}^2\right]}/{MVA_{base}} \tag{2}$$

$$I_L = {}^{S_d}/_{V_k} \tag{3}$$

$$Z_L = {}^{S_d}/_{I_L} \tag{4}$$

S_d = apparent power
I_L = current drawn by the load
Z_L = bus load impedance

With these values, the Z_L/X_{Th} index is evaluated for each load bus. The implementation iterates over all buses—up to a maximum of 30, reflecting the IEEE 30-bus test system. The custom algorithm is configured to process only load buses, as designated by code bus 0, and thus the computed index values are presented exclusively for those buses.

Step 3: Detect weakest bus:

Following the index computation, the evolutionary programming (EP) optimization algorithm is employed to configure command variables for generator buses. The weakest bus is identified by locating the load bus that yields the minimum Z_L/X_{Th} index, which is then classified as the **critical** index value, (Z_L/X_{Th}) critical index.

Step 4: Initialize the random variable:

To enhance the (Z_L/X_{Th}) critical index, the initialization phase involves generating random variables associated with generator buses. Before this step, generator bus codes are transformed into load bus codes to facilitate their integration into the simulation. After generating a set of random individuals, the resulting (Z_L/X_{Th}) critical index values are computed and used as the parent dataset for subsequent optimization iterations.

Step 5: Fitness 1 calculation:

Following the generation of the parent dataset, the first fitness evaluation—referred to as Fitness 1—is performed. This assessment quantifies the performance of each parent individual based on its effectiveness in enhancing the system's (Z_L/X_{Th}) critical index

Step 6: Mutation:

The next stage involves introducing variability through a mutation operation, implemented via a Gaussian distribution mechanism. This stochastic process perturbs the values of the random variables to produce individuals that yield improved (Z_L/X_{Th}) critical index. In this study, the mutation follows the Gaussian operator as formulated in equation (5):

$$X_{i+m,j} = X_{i+m,j} + \mathrm{N}(0, \beta(X_{jmax} + X_{jmin}))\left(\frac{f_i}{f_{max}}\right) \tag{5}$$

The new individuals resulting from this procedure are referred to as offspring.

Step 7: Fitness 2 calculation:

A second round of fitness computation—termed Fitness 2—is conducted for the offspring. Although the fitness values typically differ from those of the parent individuals, the changes may be subtle. Nevertheless, even minor alterations in the fitness scores can significantly impact the trajectory and success of the optimization process.

Step 8: Combination:

This step involves combining the original parent population (Fitness 1) with the newly generated offspring population (Fitness 2). The merged population effectively doubles the number of individuals, while maintaining consistency in the number of control variables per individual.

Step 9: Selection:

To determine the most promising solutions, the combined population is ranked in descending order according to its (ZL/X_{Th}) index values. Individuals with the highest fitness values are positioned at the top of the list. The top 50% of this sorted set—representing the best-performing individuals—are selected to serve as candidates for the next generation.

Int. Journal of Integrated Engineering Vol. 17 No. 6 (2025) p. 27-39

Step 10: Convergence test:

The convergence criterion is then evaluated to determine whether the optimization should terminate. This check is based on the difference between the highest and lowest fitness values in the current population. When this difference falls below a predefined threshold (typically 0.0001), the algorithm is considered to have converged. The threshold can be adjusted depending on the desired level of precision in the solution.

Step 11: Display Z_L/X_{Th} index results.

Upon reaching convergence, the optimal set of random variables is used to calculate the (ZL/XTh) index for all load buses in the system. These final index values reflect the system's improved stability under the optimized generator participation scheme.

3. Results and Discussion

This section presents the analysis and interpretation of the study's outcomes. Multiple test cases were examined to investigate the effects of generator participation within the ORPD framework. The insights derived from these cases are intended to assist power system operators and planners in formulating more effective future compensation strategies.

3.1 Load to Source Ratio Index for All Load Buses

Table 1 presents the initial Z_L/X_{Th} index results for all buses in the system when applied to the IEEE 30-Bus RTS. Based on the table, Bus 29 has the lowest Z_L/X_{Th} index value of 10.9667, indicating that it is the weakest bus in the IEEE-30 RTS. Other buses identified as weak due to their low Z_L/X_{Th} index values include Buses 26, 27, and 30, with corresponding values of 12.1737, 12.1737, and 17.6342, respectively, as highlighted in the table. These findings align with the results reported by Musirin et al. in [24], [25], which also identified Buses 26, 29, and 30 as weak buses in the IEEE 30-Bus RTS.

Table 1 *Load to source ratio index*

Count	Load buses	Z_L/X_{Th} index
1	3	131.6292
2	4	167.1968
3	6	198.7296
4	7	131.9920
5	9	108.0994
6	10	92.0710
7	12	104.8316
8	14	50.7085
9	15	71.5054
10	16	60.0276
11	17	68.5765
12	18	45.5842
13	19	45.7393
14	20	48.2506
15	21	72.8667
16	22	69.9013
17	23	45.0899
18	24	51.1693
19	25	30.4715
20	26	12.1737
21	27	12.1737
22	28	123.2264
23	29	10.9667
24	30	17.6342

Fig. 2 illustrates the results for voltage magnitude of all load buses before any remedial compensation initiative was taken. Voltage values a Buses 25, 26, 27 and 29 are low as can be noticed in Fig. 2. Apparently, Bus 29 exhibits the lowest voltage value which aligns with its status as a weak bus in the system. This value is very dependent on the parameters and properties of the system.

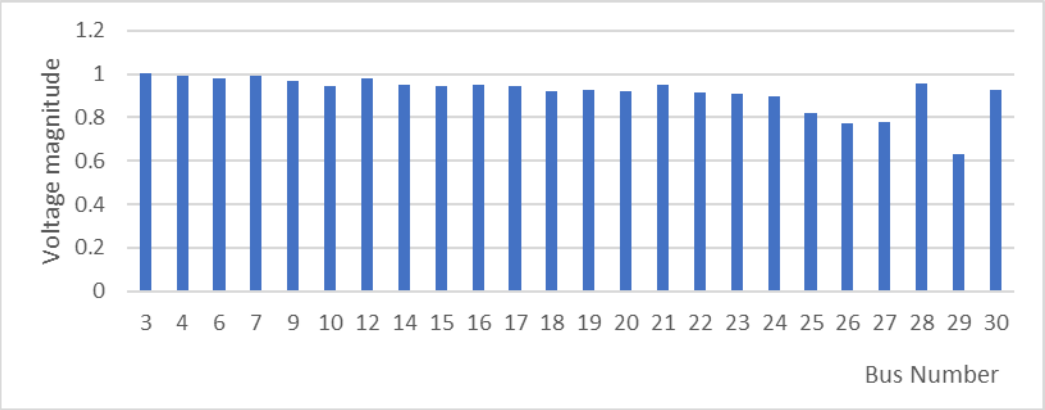

Fig. 2 *Voltage magnitude of load buses in the system*

3.2 Optimal Reactive Power Dispatch Initiative Using Evolutionary Programming

A compensation initiative was conducted in the study through the implementation of ORPD on the generator buses. Evolutionary Programming (EP) is employed to optimize the sizing of reactive power to be dispatch by the participating generators in the system. Since there are 5 generator buses in the system, not taking Bus 1 as the reference or swing bus. These buses are Buses 2, 5, 8, 11 and 13. Thus, the implementation of ORPD consider the following designated cases: -

Case A: Generator at Buses 2, 5 and 8
Case B: Generator at Buses 2, 8 and 13
Case C: Generator at Buses 8, 11 and 13
Case D: Generator at Buses 2, 5, 8, 11 and 13

3.2.1 Case A: Generator at Buses 2, 5 and 8

Table 2 tabulates the results of optimal reactive power to be dispatched at the generators at Buses 2, 5 and 8. X_2, X_5 and X_8 denote the value of reactive power to be dispatched by the generator at Buses 2, 5 and 8. Apparently, Q_{g2} = 75.3386 MVAR, Q_{g5} = 95.8262 MVAR and Q_{g8} = 90.77002 MVAR. With these amount of reactive power to be dispatched by all the three generators, the $(Z_L/X_{Th})_{critical}$ index have been increased. The implementation of ORPD involving the generators at Buses 2, 5 and 8 managed to improve the $(Z_L/X_{Th})_{critical}$ index from 10.9667 to 17.8169 for Bus 29. This implementation has also increased all the index values for all load buses in the system as shown in the table. This implies that ORPD initiative using EP has improved the indexed values at all buses, which in turn has improved the voltage level at all buses in the system. This phenomenon can be observed in Fig. 3. In general, ORPD implementation has managed to restore the system collapse indicated by the improvement of voltage values at all buses in the system.

Int. Journal of Integrated Engineering Vol. 17 No. 6 (2025) p. 27-39

Table 2 *Index values for all load buses*

	Before ORPD Implementation		After ORPD Implementation	
Count	Load buses	Z_L/X_{Th} index	Load buses	Z_L/X_{Th} index
1	3	131.6292	3	141.7051
2	4	167.1968	4	182.1982
3	6	198.7296	6	219.8362
4	7	131.9920	7	156.9983
5	9	108.0994	9	123.5936
6	10	92.0710	10	106.4829
7	12	104.8316	12	118.0894
8	14	50.7085	14	58.5014
9	15	71.5054	15	82.3477
10	16	60.0276	16	69.4066
11	17	68.5765	17	80.0485
12	18	45.5842	18	53.4875
13	19	45.7393	19	53.9371
14	20	48.2506	20	56.8199
15	21	72.8667	21	84.5934
16	22	69.9013	22	81.9593
17	23	45.0899	23	53.4573
18	24	51.1693	24	61.7050
19	25	30.4715	25	38.8653
20	26	12.1737	26	16.5663
21	27	12.1737	27	40.2899
22	28	123.2264	28	144.4397
23	29	10.9667	29	17.8169
24	30	17.6342	30	21.6119
x_2	x_5	x_8	$(Z_L/X_{Th})_{critical}$	
75.3386	95.8262	90.77002	17.8169	

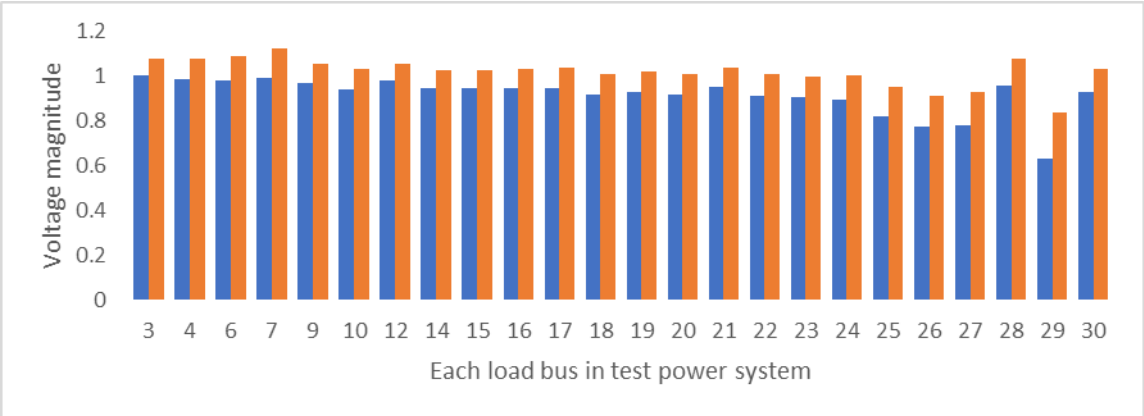

Fig. 3 *Voltage magnitude before and after the implementation or ORPD involving generatorat Buses 2, 5 and 8 using EP*

3.2.2 Case B: Generator at Buses 2, 8, 13

A further analysis was conducted on the system, as simulated in Case B, where ORPD was applied to the generators located at Buses 2, 8, and 13. The results, presented in Table 3, demonstrate that implementing ORPD at these generators successfully enhanced the system's index value. Table 3 provides the optimal reactive power

dispatch values for generators at Buses 2, 8, and 13, denoted as X_2, X_8, and X_{13}, respectively. Specifically, the dispatched reactive power values are Q_{g2} = 69.9088 MVAR, Q_{g8} = 97.3216 MVAR, and Q_{g13} = 84.8976 MVAR. With these reactive power adjustments, the $(Z_L/X_{Th})critical$ index increased from 10.9667 to 17.5460. Additionally, all load bus index values in the system improved, as reflected in the table. This confirms that the ORPD strategy utilizing EP effectively enhanced the index values across all buses, leading to an overall improvement in system voltage levels. The impact of this improvement is illustrated in Fig. 4. In summary, the ORPD implementation successfully mitigated system collapse, as evidenced by the enhanced voltage levels across all buses in the system.

Table 3 *Index values for all load buses*

	Before ORPD Implementation		After ORPD Implementation	
Count	Load buses	Z_L/X_{Th} index	Load buses	Z_L/X_{Th} index
1	3	131.6292	3	140.0905
2	4	167.1968	4	179.5904
3	6	198.7296	6	213.1804
4	7	131.9920	7	140.2361
5	9	108.0994	9	123.8829
6	10	92.0710	10	109.2028
7	12	104.8316	12	132.2949
8	14	50.7085	14	65.1213
9	15	71.5054	15	90.4119
10	16	60.0276	16	75.1562
11	17	68.5765	17	83.7175
12	18	45.5842	18	57.5734
13	19	45.7393	19	57.3586
14	20	48.2506	20	59.7861
15	21	72.8667	21	87.2800
16	22	69.9013	22	84.3152
17	23	45.0899	23	57.5547
18	24	51.1693	24	64.3141
19	25	30.4715	25	39.2808
20	26	12.1737	26	16.7464
21	27	12.1737	27	39.2808
22	28	123.2264	28	139.7870
23	29	10.9667	29	17.5460
24	30	17.6342	30	21.4228
X_2	X_8	X_{13}	$(Z_L/X_{Th})_{critical}$	
69.9088	97.3216	84.8976	17.5460	

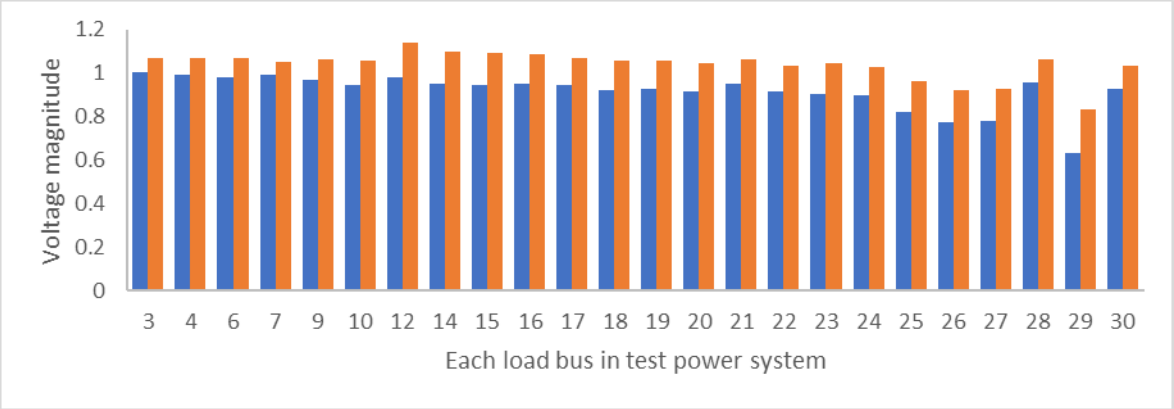

Fig. 4 *Voltage magnitude before and after the implementation of ORPD involving generator at Buses 2, 8, 13 using EP*

Int. Journal of Integrated Engineering Vol. 17 No. 6 (2025) p. 27-39

3.2.3 Case C: Generator at Buses 8, 11, 13

Additional investigation was carried out to the system as simulated in Case C, which included ORPD actions on generators at Buses 8, 11 and 13. The outcomes are summarized in Table 4, illustrating the system's enhance performance resulting from the ORPD initiative targeting generators at Buses 8, 11 and 13. X_8, X_{11} and X_{13} denote the values of reactive power to be dispatched at the generator at buses 8, 11 and 13. Apparently, Q_{g8} = 75.3386 MVAR, Q_{g11} = 95.8262 MVAR and Q_{g13} = 90.7700 MVAR. By dispatching the specified reactive power amounts from all three generators, the $(Z_L/X_{Th})_{critical}$ index has experienced an increase. The execution of ORPD involving generators at Buses 2, 8, and 13 has been maximized by the $(Z_L/X_{Th})_{critical}$ index from 10.9667 to 19.1596. This implementation has also elevated the index values for all load buses within the system, as depicted in Table 4. Consequently, the ORPD initiative employing EP has enhanced the indexed values at all buses, ultimately resulting in improved voltage levels throughout the system. This observable effect is illustrated in Fig. 5. In summary, the implementation of ORPD has effectively mitigated the risk of system collapse, as indicated by the enhanced voltage values across all buses in the system.

Table 4 *Index values for all load buses*

Count	Before ORPD Implementation		After ORPD Implementation	
	Load buses	Z_L/X_{Th} index	Load buses	Z_L/X_{Th} index
1	3	131.6292	3	144.8759
2	4	167.1968	4	186.7810
3	6	198.7296	6	223.3842
4	7	131.9920	7	144.9920
5	9	108.0994	9	145.0566
6	10	92.0710	10	123.5815
7	12	104.8316	12	142.6998
8	14	50.7085	14	70.7275
9	15	71.5054	15	98.6166
10	16	60.0276	16	82.8836
11	17	68.5765	17	94.2827
12	18	45.5842	18	63.8408
13	19	45.7393	19	64.1635
14	20	48.2506	20	67.1074
15	21	72.8667	21	100.0122
16	22	69.9013	22	95.0529
17	23	45.0899	23	63.4308
18	24	51.1693	24	71.5446
19	25	30.4715	25	42.7953
20	26	12.1737	26	18.4419
21	27	12.1737	27	42.6458
22	28	123.2264	28	145.3068
23	29	10.9667	29	19.1596
24	30	17.6342	30	23.0179
X_8	X_{11}	X_{13}	$(Z_L/X_{Th})_{critical}$	
75.3386	95.8262	90.7700	19.1596	

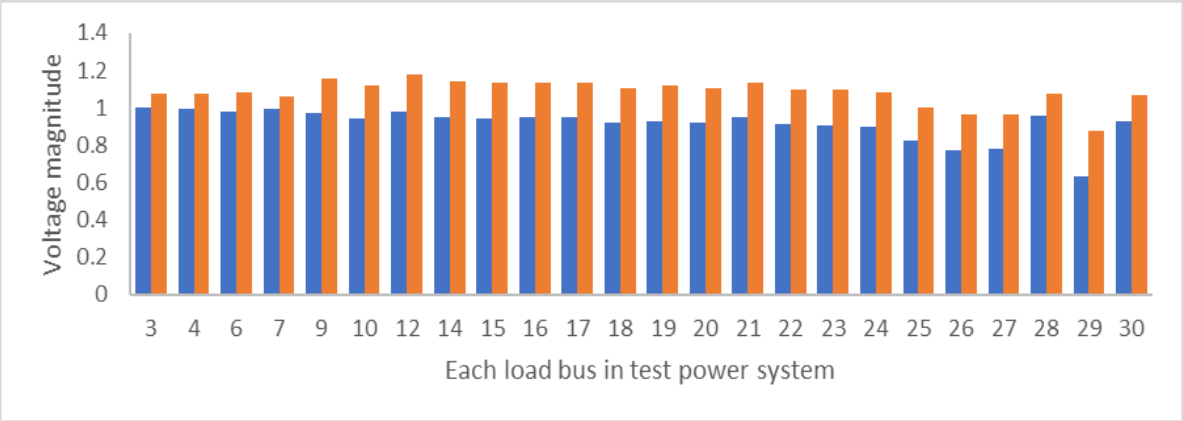

Fig. 5 *Voltage magnitude before and after the implementation of ORPF involving generator at Buses 8, 11, 13 using EP*

3.2.4 Case D: Generator at buses 2, 5, 8, 11 and 13

Table 5 presents the findings related to the optimal allocation of reactive power for generators at Buses 2, 5, 8, 11 and 13. X_2, X_5, X_8, X_{11} and X_{13} are denotes the reactive power to be dispatched by the respective generators at those respective busses. Notably, Q_{g2} is recorded at 79.2351 MVAR, Q_{g5} at 64.9600 MVAR, Q_{g8} at 82.0714 MVAR, Q_{g11} at 94.6192 MVAR and Q_{g13} at 85.7319 MVAR. With these reactive power settings across five generators, there has been an increase in the $(Z_L/X_{Th})_{critical}$ index to 24.3144. The ORPD implementation involving generators at buses 2, 5, 8, 11 and 13 has effectively elevated the $(Z_L/X_{Th})_{critical}$ index from 10.9667 to 24.3144 for Bus 29. Furthermore, this implementation has led to increased index values for all load buses within the system, as illustrated in Table 5. This indicates that the ORPD initiative employing EP has enhanced the indexed values across all buses, subsequently improving voltage levels throughout the entire system. This observable effect is depicted in Fig. 6. In summary, the implementation of ORPD has effectively mitigated the risk of system collapse, as evidenced by the improved voltage values at all buses within the system.

Table 5 *Index values for all load buses*

Count	Before ORPD Implementation		After ORPD Implementation	
	Load buses	Z_L/X_{Th} index	Load buses	Z_L/X_{Th} index
1	3	131.6292	3	158.5934
2	4	167.1968	4	208.2696
3	6	198.7296	6	253.6145
4	7	131.9920	7	176.9980
5	9	108.0994	9	166.1448
6	10	92.0710	10	142.1396
7	12	104.8316	12	162.1199
8	14	50.7085	14	81.0881
9	15	71.5054	15	112.9914
10	16	60.0276	16	95.1389
11	17	68.5765	17	108.8992
12	18	45.5842	18	73.7855
13	19	45.7393	19	74.4238
14	20	48.2506	20	77.7160
15	21	72.8667	21	115.1024
16	22	69.9013	22	109.8267
17	23	45.0899	23	73.6189
18	24	51.1693	24	83.7802
19	25	30.4715	25	51.2305
20	26	12.1737	26	22.7063
21	27	12.1737	27	51.3750

Int. Journal of Integrated Engineering Vol. 17 No. 6 (2025) p. 27-39

Count	Before ORPD Implementation		After ORPD Implementation	
	Load buses	Z_L/X_{Th} index	Load buses	Z_L/X_{Th} index
22	28	123.2264	28	168.3052
23	29	10.9667	29	24.3144
24	30	17.6342	30	27.5546

X_2	X_5	X_8	X_{11}	X_{13}	$(Z_L/X_{Th})_{critical}$
79.2351	64.9600	82.0714	94.6192	85.7319	24.3144

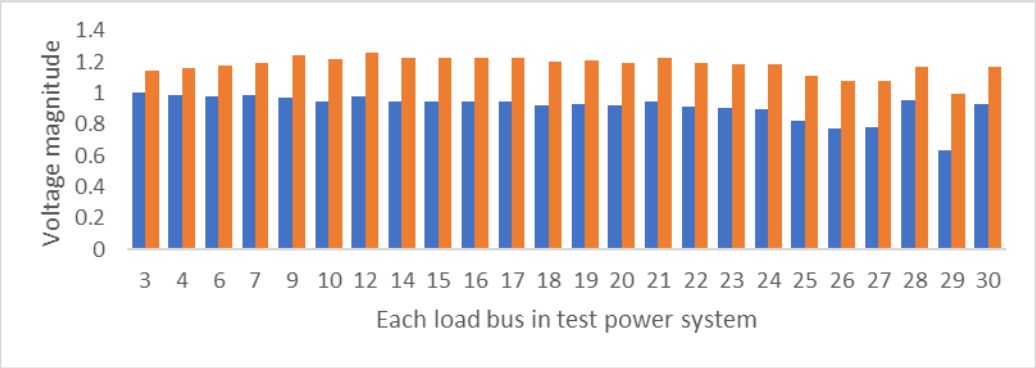

Fig. 6 *Voltage magnitude before and after optimised*

Maximizing the Z_L/X_{Th} index has effectively enhanced voltage levels at the load buses, particularly at the weakest bus, by strategically selecting specific generator buses, thereby improving voltage security. As illustrated in Fig. 7, the highest voltage magnitude at Bus 29 is achieved when all five generator buses are considered as random variables. This is because, in Case D, the system operates at full capacity to ensure power supply to all load buses.

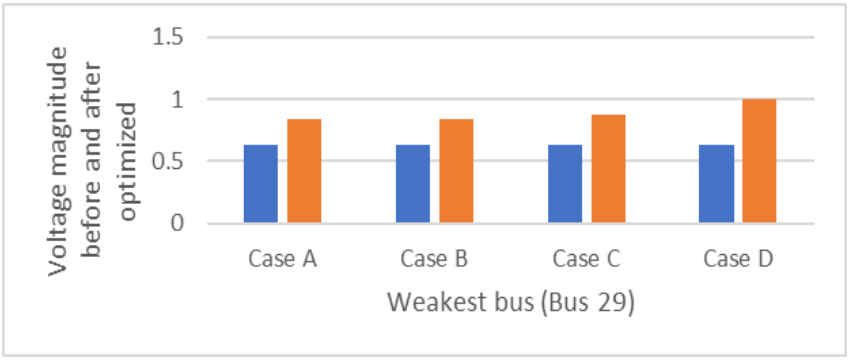

Fig. 7 *Voltage magnitude of weakest bus*

4. Conclusion

This paper introduces a computational intelligence approach combined with a load-to-source ratio index-based technique for voltage security restoration. Evolutionary Programming (EP) is employed to identify the weakest bus in the system under various load scenarios. The identification process involves calculating the $\boldsymbol{Z_L/X_{Th}}$ index. Once a specific load is set, the load-to-source index for each bus is determined. Upon identifying the weakest load bus, EP is utilized to optimize the ORPD across the generators of the buses, thereby maximizing the critical index. This enhancement of the $\boldsymbol{Z_L/X_{Th}}$ index effectively restores the voltage magnitude at the load bus.

Acknowledgement

The authors acknowledge Ministry of Higher Education Malaysia (MOHE) for funding under Fundamental Research Grant (FRGS) number code: FRGS/1/2019/ TK04/UITM/01/1 and 600-IRMI/FRGS 5/3 (381/2019).

Conflict of Interest

Authors declare that there is no conflict of interests regarding the publication of the paper.

Author Contribution

The authors confirm contribution to the paper as follows: ***study conception and design:*** Muhammad Naqiyuddin Ismail*,* Ismail Musirin*;* ***data collection:*** Muhammad Naqiyuddin*;* ***analysis and interpretation of results:*** Ismail Musirin, Vinothini Kasinathan, Aida Mustapha*;* ***draft manuscript preparation:*** Muhammad Naqiyuddin Ismail, Mazliza Abdul Halim, Ismail Musirin, Habibah Zulkefle*. All authors reviewed the results and approved the final version of the manuscript.*

References

[1] Zin, A. a. M., & Karim, S. P. A. (2013). Protection system analysis using fault signatures in Malaysia. *International Journal of Electrical Power & Energy Systems, 45*(1), 194-205. https://doi.org/10.1016/j.ijepes.2012.08.025

[2] Alhelou, H. H., Hamedani-Golshan, M. E., Njenda, T. C., & Siano, P. (2019). A survey on power system blackout and cascading Events: Research Motivations and challenges. *Energies, 12*(4), 682. https://doi.org/10.3390/en12040682

[3] Wang, S., & Chiang, H. (2016). Multi-objective service restoration of distribution systems using user-centered methodology. *International Journal of Electrical Power & Energy Systems, 80*, 140–149. https://doi.org/10.1016/j.ijepes.2016.01.021

[4] Liao, S., Yao, W., Han, X., Fang, J., Ai, X., Wen, J., & He, H. (2019). An improved two-stage optimization for network and load recovery during power system restoration. *Applied Energy, 249*, 265–275. https://doi.org/10.1016/j.apenergy.2019.04.176

[5] Shen, C., Kaufmann, P., Hachmann, C., & Braun, M. (2018). Three-stage power system restoration methodology considering renewable energies. *International Journal of Electrical Power & Energy Systems, 94*, 287–299. https://doi.org/10.1016/j.ijepes.2017.07.007

[6] Esmaili, M. R., Khodabakhshian, A., Hooshmand, R., & Siano, P. (2018). A new coordinated design of sectionalizing scheme and load restoration process considering reliability of transmission system. *International Journal of Electrical Power & Energy Systems, 102*, 23–37. https://doi.org/10.1016/j.ijepes.2018.04.017

[7] Borges, T. T., Carneiro, S., Garcia, P., & Pereira, J. (2016). A new OPF based distribution system restoration method. *International Journal of Electrical Power & Energy Systems, 80*, 297–305. https://doi.org/10.1016/j.ijepes.2016.01.024

[8] Ko, B. J., Lee, G., Choi, K., & Kim, R. (2019). A coordinated droop control method using a virtual voltage axis for power management and voltage restoration of DC microgrids. *IEEE Transactions on Industrial Electronics, 66*(11), 9076–9085. https://doi.org/10.1109/tie.2018.2877135

[9] Wang, F., Xiao, X., Sun, Q., Chen, C., Chen, S., & Fan, J. (2019). Service restoration for distribution network with DGs based on stochastic response surface method. *International Journal of Electrical Power & Energy Systems*, *107*, 557–568. https://doi.org/10.1016/j.ijepes.2018.12.015

[10] Jiang, Y., Chen, S., Liu, C., Sun, W., Luo, X., Liu, S., Bhatt, N., Uppalapati, S., & Forcum, D. (2017). Blackstart capability planning for power system restoration. *International Journal of Electrical Power & Energy Systems*, *86*, 127–137. https://doi.org/10.1016/j.ijepes.2016.10.008.

[11] Ketabi, A., Karimizadeh, A., & Shahidehpour, M. (2019). Optimal generation units start-up sequence during restoration of power system considering network reliability using bi-level optimization. *International Journal of Electrical Power & Energy Systems*, *104*, 772–783. https://doi.org/10.1016/j.ijepes.2018.07.045

[12] Ye, J., Gooi, H. B., Wang, B., Li, Y., & Liu, Y. (2019). Elliptical restoration based single-phase dynamic voltage restorer for source power factor correction. *Electric Power Systems Research*, *166*, 199–209. https://doi.org/10.1016/j.epsr.2018.10.011.

[13] Renner, R. H., & Van Hertem, D. (2016). Potential of using DC voltage restoration reserve for HVDC grids. *Electric Power Systems Research*, *134*, 167–175. https://doi.org/10.1016/j.epsr.2016.01.006

[14] Hashemi, S. R., Aghamohammadi, M. R., & Sangrody, H. (2018). Restoring desired voltage security margin based on demand response using load-to-source impedance ratio index and PSO. *International Journal of Electrical Power & Energy Systems*, *96*, 143–151. https://doi.org/10.1016/j.ijepes.2017.09.044

[15] Tobón, J. E., RamíRez, J. M., & Correa, R. E. (2015). Tracking the maximum power transfer and loadability limit from sensitivities-based impedance matching. *Electric Power Systems Research*, *119*, 355–363. https://doi.org/10.1016/j.epsr.2014.10.013.

[16] Li, W., Chen, T., & Xu, W. (2010). On impedance matching and maximum power transfer. *Electric Power Systems Research*, *80*(9), 1082–1088. https://doi.org/10.1016/j.epsr.2010.01.015

[17] F. Wang, et al., "Voltage Control Embedded Resilient Distribution System Restoration," *IEEE Transactions on Power Systems*, 2023.

[18] Karaman, A., Pacal, I., Baştürk, A., Akay, B., Nalbantoğlu, U., Coskun, S., Sahin, O., & Karaboğa, D. (2023). Robust real-time polyp detection system design based on YOLO algorithms by optimizing activation functions and hyper-parameters with artificial bee colony (ABC). *Expert Systems With Applications*, *221*, 119741. https://doi.org/10.1016/j.eswa.2023.119741

[19] Cui, Y. (2023). Optimizing decision trees for English Teaching Quality Evaluation (ETQE) using Artificial Bee Colony (ABC) optimization. *Heliyon*, *9*(8), e19274. https://doi.org/10.1016/j.heliyon.2023.e19274

[20] Ettappan, M., Vimala, V., Ramesh, S., & Kesavan, V. T. (2020). Optimal reactive power dispatch for real power loss minimization and voltage stability enhancement using Artificial Bee Colony Algorithm. *Microprocessors and Microsystems*, *76*, 103085. https://doi.org/10.1016/j.micpro.2020.103085

[21] M. Alhuyi Nazari, "A Comprehensive Review on the Role of Artificial Intelligence in Power System Stability, Control, and Protection," Applied Sciences, vol. 14, no. 14, pp. 6214, 2024. DOI: 10.3390/app14146214.

[22] Saddique, M. S., Bhatti, A. R., Haroon, S. S., Sattar, M. K., Amin, S., Sajjad, I. A., Haq, S. S. U., Awan, A. B., & Rasheed, N. (2020). Solution to optimal reactive power dispatch in transmission system using meta-heuristic techniques—Status and technological review. *Electric Power Systems Research, 178*, 106031. https://doi.org/10.1016/j.epsr.2019.106031

[23] Nuaekaew, K., Artrit, P., Pholdee, N., & Bureerat, S. (2020). Optimal reactive power dispatch problem using a two-archive multi-objective grey wolf optimizer. *Expert Systems With Applications*, vol. *87*, pp79–89. https://doi.org/10.1016/j.eswa.2017.06.009

[24] Mei, R. N. S., Sulaiman, M. H., Mustaffa, Z., & Daniyal, H. (2017). Optimal reactive power dispatch solution by loss minimization using moth-flame optimization technique. *Applied Soft Computing*, *59*, 210–222. https://doi.org/10.1016/j.asoc.2017.05.057

[25] Hamid, Z. A., & Musirin, I. (2014). Optimal Fuzzy Inference System incorporated with stability index tracing: An application for effective load shedding. *Expert Systems with Applications*, *41*(4), 1095–1103. https://doi.org/10.1016/j.eswa.2013.07.105

[26] Elsakaan, A. A., El-Sehiemy, R. A., Kaddah, S. S., & El-Said, M. (2018). An enhanced moth-flame optimizer for solving non-smooth economic dispatch problems with emissions. *Energy*, *157*, 1063–1078. https://doi.org/10.1016/j.energy.2018.06.088

[27] Prada, R., Palomino, E., Pilotto, L., & Bianco, A. (2005). Weakest bus, most loaded transmission path and critical branch identification for voltage security reinforcement. *Electric Power Systems Research*, *73*(2), 217–226. https://doi.org/10.1016/j.epsr.2004.08.006